AerospaceEurope Conference2020
BORDEAUX, FRANCE | 25 - 28 FEBRUARY 2020
CEAS Council of European Aerospace Societies
HOSTED BY: 3AF Association Aéronautique et Astronautique de France

Paper ID: #464

EVALUATION OF THERMAL COMFORT FOR NOVEL AIRCRAFT CABIN VENTILATION CONCEPTS

Daniel Schmeling* [(1)], Andrey Shishkin [(1)], Tobias Dehne [(1)], Pascal Lange [(1)], Ingo Gores [(2)]

*[(1)] German Aerospace Center (DLR), Institute of Aerodynamics and Flow Technology, Bunsenstraße 10, 37073 Göttingen, Germany, *Email: daniel.schmeling@dlr.de*
[(2)] Airbus Operations GmbH, Kreetslag 10, 21129 Hamburg, Germany, Email: ingo.gores@airbus.com

KEYWORDS: Aircraft Cabin, Ventilation Concepts, Passenger's Thermal Comfort, Energy Efficiency, Numerical Simulations

ABSTRACT:

To analyse promising ventilation concepts regarding outlet and exhaust dimensions and locations as well as momentum and temperature of the inflowing air, numerical simulations are performed. The steady state (RANS) numerical simulations are based on second-order finite volume schemes. In a post-processing tool chain, thermal comfort-related quantities, such as predicted percentage of dissatisfied (PPD) and predicted mean vote (PMV) are calculated. Further, the local mean age of air is computed. The test configuration is a slightly simplified Airbus A350 geometry with nine-abreast seating. The computational domain spans five rows with adiabatic, non-permeable boundary conditions in flight direction.

Several ventilation concepts are analysed with respect to their heat removal efficiency and thermal comfort. Differences regarding the temperature stratification and the local mean age of air are detected. Further, different locations and dimensions of the supply and exhaust air openings result in locally different flow fields. Here, promising locations providing a good overall comfort are detected.

1. INTRODUCTION

Flexible cabin layout, high demands on thermal comfort and energy efficiency as well as industrial modular design are the main challenges for aircraft engineers when addressing the ventilation of the aircraft cabin. Nowadays, mixing ventilation is installed in all commercial aircraft, guaranteeing a high degree of mixing and therefore a robust and stable ventilation concept for the cabin [1]. However, complex and weight-intensive ducts are required. In addition, the system provides only limited heat removal efficiency and high velocities are prone to cause draft on single seats [2]. In order to address these challenges, novel ventilation concepts are investigated within the scope of the ADVENT project - Advanced ventilation techniques for modern long-range passenger aircraft to promote future energy management systems.

2. NUMERICAL APPROACH

The numerical simulations are carried out using the high-performance computing (HPC) cluster of the Institute of Aerodynamics and Flow Technology in Göttingen. The commercial edition Engys of the open source computational fluid dynamics (CFD) toolkit OpenFOAM is used to perform the calculations and for the pre- and post-processing operations.

2.1. Numerical Scheme

The governing equations are Navier-Stokes equations with Boussinesq approximation:

$$\nabla \cdot \boldsymbol{u} = 0, \tag{1}$$

$$\frac{\partial \boldsymbol{u}}{\partial t} + (\boldsymbol{u} \cdot \nabla \boldsymbol{u}) = \nu \nabla^2 \boldsymbol{u} - \frac{1}{\rho_0} \nabla p + \boldsymbol{g} \beta \theta, \tag{2}$$

$$\frac{\partial \theta}{\partial t} + (\boldsymbol{u} \cdot \nabla \boldsymbol{u}) = \kappa \nabla^2 \theta, \tag{3}$$

where ρ_0 is the reference density, $\theta = T - T_0$ is the deviation of temperature from the reference value T_0, β is the coefficient of thermal expansion, κ is the thermal conductivity coefficient and $\boldsymbol{g}$ represents the gravity vector. Eqs (1) - (3) describe buoyancy-driven flow provided that the thermal expansion coefficient and temperature variance are small enough:

$$\beta\theta \ll 1. \tag{4}$$

The radiation transfer is computed using the Finite Volume Discrete Ordinates Method (fvDOM) implemented in OpenFOAM to solve the radiation transfer equation (RTE) for a predefined number of directions in the ambient media.
The thermal radiation transfer equation for a gray medium in a general form reads [3]:

$$\frac{\partial I}{\partial s} + (\alpha + \sigma_s) I = \alpha I_b + \frac{\sigma_s}{4\pi} \int_{4\pi} I(s_i) \Phi(s_i, \boldsymbol{s}) d\Omega_i \,, \quad (5)$$

where $I = I(\boldsymbol{x}, \boldsymbol{s})$ is the radiation intensity at position $\boldsymbol{x}$ along direction $\boldsymbol{s}$, $I_b = I_b(\boldsymbol{x})$ is the black body radiation intensity, $\Phi(s_i, \boldsymbol{s}) = \Phi(\boldsymbol{x}, s_i, \boldsymbol{s})$ is the scattering phase function, $\alpha = \alpha(\boldsymbol{x})$ and $\sigma_s = \sigma(\boldsymbol{x}, \boldsymbol{s})$ are absorption and scattering coefficients, respectively. Since the air is treated as non-participating and non-scattering medium in the simulations, the calculation of Eq. (5) is reduced accordingly.
For the diffusively emitting and reflecting wall boundaries, the following conditions are valid [3]:

$$I(\boldsymbol{s}) = \varepsilon I_b + \frac{1-\alpha}{\pi} \int_{(\boldsymbol{n}\cdot\boldsymbol{s})<0} I(\boldsymbol{s}') |\boldsymbol{n} \cdot \boldsymbol{s}'| d\Omega', \quad (6)$$

where ε is the emissivity coefficient and $\boldsymbol{n}$ is an outer normal-to-surface element. The radiative heat flux calculated on the walls,

$$q_r = \int I(\boldsymbol{s})(\boldsymbol{n} \cdot \boldsymbol{s}) d\Omega, \quad (7)$$

is further applied as radiative component of the total heat flux in the boundary conditions of Eq. (3). The standard OpenFOAM steady state solver buoyantBoussinesqSimpleFoam is used to solve the system of Eqs. (1) - (3). It is based on the classical SIMPLE algorithm (Semi-Implicit Method for Pressure-Linked Equations), initially developed by Patankar and Spalding [4]. The solver allows for the simulation of a variety of turbulence models, here we use the k-ω-SST turbulence model. Thanks to the fine resolution in the vicinity of the walls, the low Reynolds number approach (Low-Re) can be used for near-wall turbulence modeling by applying the following conditions:

- k = 10^{-16} (very small number, not modeled),
- omegaWallFunction for omega (standard ω wall function),
- kinematic turbulent viscosity nut is calculated (not modeled).

Usually, the use of Low-Re conditions leads to an essential improvement of the accuracy of the simulations if they are applied at a well-resolved wall ($y+< 5$).

2.2. CAD Preparation/Computational Domain

The test configuration is a slightly simplified Airbus A350 geometry with nine-abreast seating. The computational domain spans five rows with adiabatic, non-permeable boundary conditions in flight direction, see Fig. 1.

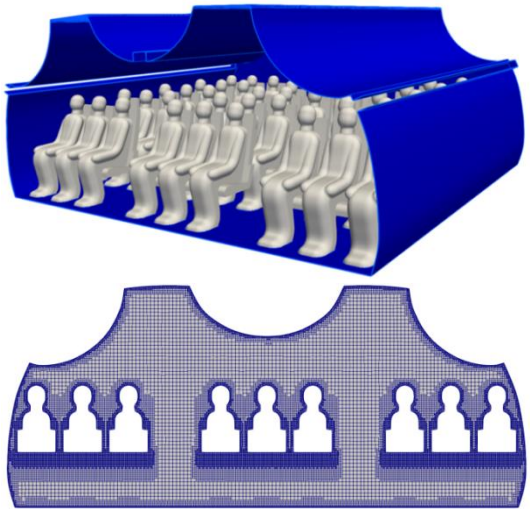

Figure 1. Computational domain

2.3. Thermal Manikins

For the simulation of the blockage and the heat release of sitting passengers, thermal manikins are employed.
To reduce the computational costs by decreasing the mesh size, we reduce the details of the manikins from the complex manikin (Fig. 2, left) to the simplified manikin (Fig. 2, right).

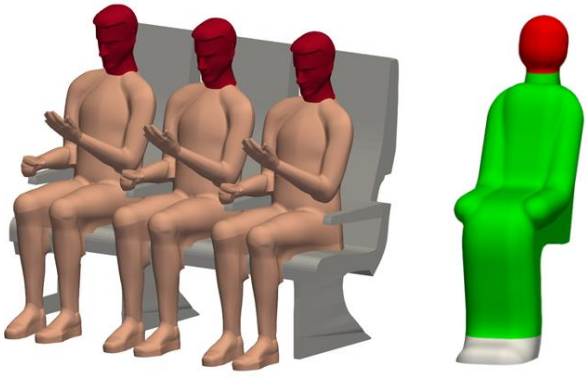

Figure 2. Thermal manikins. Left: complex version with many details. Right: simplified manikin for faster simulations and reduced computational costs

The geometry of the passenger dummies and seats and their thermal boundary conditions are

the same for all configurations. The thermal boundary conditions are as follows:

- head - 83.87 W/m² (heat flux density),
- body - 50.32 W/m² (heat flux density),
- seat - 0 W/m² (adiabatic)

The dummy's total heat flux is equal to 75 W.

2.4. Post-Processing of Thermal Comfort

In a post-processing tool chain, thermal comfort quantities, such as predicted percentage of dissatisfied (PPD) and predicted mean vote (PMV) are calculated.

Predicted Mean Vote
The predicted mean vote (PMV) is the complex comfort index which reflects the human response to the local thermal environment [5]. It takes into account both physical environment parameters and individual human properties:

- air temperature and velocity
- mean radiant temperature
- relative humidity
- metabolic rate
- physical activity
- clothing insulation

The PMV model is based on a series of experiments carried out by P.O. Fanger in the 1970s involving a large group of subjects exposed to a variety of controlled environments. The results of the measurements were evaluated using the 7-point thermal sensation, and then processed statistically with respect to the basic heat balance equation [6].

Predicted Percentage of Dissatisfied
The PPD is an index that establishes a quantitative prediction of the percentage of thermally dissatisfied people who feel too cool or too warm [5]. In Eq. (8) it is related to the PMV index discussed in the previous section:

$$PPD = 100 - 95 \cdot exp(-0.03353 \cdot PMV^4 - 0.2179 \cdot PMV^2) \quad (8)$$

Draught Rate
Draught is an unwanted local cooling of the body caused by air movements and is considered to be one of the most important local discomfort factors [5]. The comfort index of the draught rate (DR) is defined as the percentage of people predicted to be bothered by draught. The semi-empirical formula (Eq. (9))

$$DR = (34 - T) \cdot (U - 0.05)^{0.62} \cdot (0.37 \cdot Tu \cdot U + 3.14) \quad (9)$$

was developed by Fanger et al. [7] based on a series of experiments with fifty subjects, dressed to experience a neutral thermal sensation under different conditions of mean velocity U and turbulence intensity Tu.

Operative Temperature
The operative temperature T_{op} is defined as uniform temperature of an imaginary black enclosure in which an occupant would exchange the same amount of heat by radiation and convection as in the actual non-uniform environment [5].

2.4. Post-Processing of Age Of Air

Further, the local mean age of air is computed by means of a passive scalar solver implemented in Engys [8]. The second-order equation for the local age of air Θ (Bartak et al. [9]) reads (Eq. (10)):

$$\nabla \cdot \left[(\rho \boldsymbol{u} T_{AoA}) - \left(\frac{\mu}{Sc} + \frac{\mu_t}{Sc_t} \right) \nabla T_{AoA} \right] = 1 \quad (10)$$

Here $\boldsymbol{u}$ is the velocity, ρ is the density of air, μ and μ_t are the physical and turbulent viscosities, Sc and Sc_t are the laminar and turbulent Schmidt numbers, respectively.

2.5. Visualisations

The investigated ventilation concepts are presented in terms of temperature and velocity distributions, local comfort parameters as well as age of air for cross-sections in the middle of the numerical domain, i.e., cutting the third seat row. Further, velocity and temperature fields are presented for longitudinal cross-sections in the centre of the cabin. Global parameter such as heat removal efficiency are calculated using the mean temperatures of the inflowing and outflowing air as well as the volume-averaged mean temperature in the part of the cabin that is not occupied by passengers.
The heat removal efficiency serves as a measure to evaluate the capability of the ventilation concept to remove heat from the cabin. It is defined

according to [10] by the temperature of the inflowing air T_{in}, the temperature of the exhaust $T_{exhaust}$ and the mean cabin temperature T_{cabin}, see Eq. (11).

$$HRE = 0.5 \cdot \frac{T_{exhaust} - T_{in}}{T_{cabin} - T_{in}} \qquad (11)$$

In accordance with this definition, a ventilation concept with perfect mixing of the air in the cabin, that is $T_{exhaust} = T_{cabin}$, has a heat removal efficiency of 0.5. However, state-of-the-art mixing ventilation, which is typically installed in passenger cabins of aircraft, has even lower values of about 0.4 [2].

3. VENTILATION CONCEPTS

The investigation of the novel ventilation concepts is motivated by many different factors:

- Increasing the HRE (to allow for higher heat load densities)
- Allowing for modular aircraft design and construction
- Providing thermal comfort for passengers
- High air quality (e.g. by low local age of air)

With regard to the first point, the new concepts are compared to state-of-the-art mixing ventilation with a HRE of around 0.4 [2]. The higher HRE could result in a decreased sizing of the climate pack and thus reduced weight; or on the other hand, allow for higher heat load densities in the cabin, i.e. more passengers.
The modular aircraft design is of special interest for a simplified construction process using pre-assembled modules which already contain the cabin ventilation systems. Therefore, the presented ventilation concepts are – at least partially – fully integrated in single modules, e.g. crown or sidewall modules. Within these considerations, simple installation, pre-defined connections and reduced pipe lengths are additional advantages.
The latter two bullet points are of great importance for the acceptance of novel concepts by the passengers and the cabin crew. Further, a low local mean age of air helps to decrease the airborne spreading of infectious diseases within the cabin.

3.1. Ceiling-Based Concepts

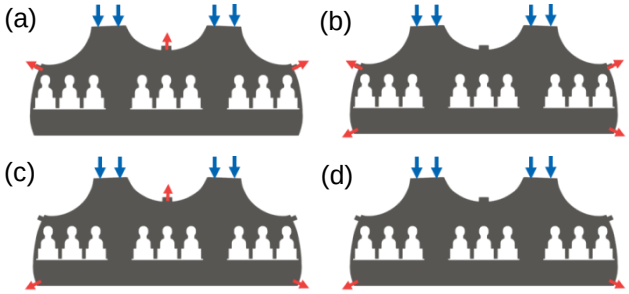

Figure 3. Ceiling-based concepts with fresh air supply in the ceiling and different exhaust configurations.

The presented ceiling-based ventilation concepts use small micro-jets for the air supply and the inlet area spans the whole ceiling area above the aisles. This kind of air supply is well known from trains, especially from long-distance trains, such as the German Inter City Express (ICE) [11]. Some results including objective and subjective evaluations were obtained in a generic train laboratory equipped with this air supply system [12]. In both cases, the generic train laboratory and the long-distance train in-operation, the results proved the applicability and the robustness of this ventilation system. In contrast to the discussed experimental studies, we realised the micro-jet holes for this numerical study by square holes simplifying the mesh generation. Different exhaust configurations are analysed: lateral and central (a), lateral and dado (b), central and dado (c) as well as solely dado (d), also summarized in Tab. 1.

Table 1. Parameter for ceiling-based ventilation.

Case	Exhaust 1	Exhaust 2
(a)	Lateral 67%	Central 33%
(b)	Lateral 67%	Dado 33%
(c)	Central 67%	Dado 33%
(d)	Dado 100%	---

3.2. Floor-Based Concept

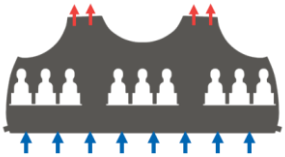

Figure 4. Floor-based concept with fresh air supply through the floor.

In contrast to the ceiling-based ventilation concept, where the fresh air is supplied through the ceiling

area, we use the whole floor area for the floor-based ventilation concepts (Fig. 4). The concept of using the entire floor is a result of the simplified mesh generation and the simplified definition of the numerical boundary conditions. In experimental applications or even in a possible implementation in a real aircraft, this floor-based ventilation will be realised by a local, low-momentum air distribution system below the seats. This technique has already been successfully applied in a ground-based research aircraft Do728 [2] as well as in test flights with an A320 ATRA [13]. The exhaust is implemented in the ceiling of the cabin. The main advantage of the concept is the extremely high heat removal efficiency, which is more than twice as good as for state-of-the-art mixed convection [2]. However, the cold fresh air on floor level results in strong vertical temperature gradients, which are likely to be uncomfortable for the passengers.

3.3. Sidewall-Based Concepts

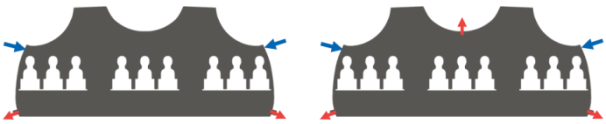

Figure 5. Sidewall-based concepts with fresh air supply in the lateral sidewall and different exhaust configurations.

The last group of presented ventilation concepts is called sidewall-based concepts, where the air is supplied by micro-jets integrated in the lateral parts of the cabin. The exhaust is installed in the dado panels solely (Fig. 5, left) or implemented as a combination of dado and central exhausts (Fig. 5, right).

4. RESULTS and DISCUSSION

In this chapter, we will first discuss one ventilation concept in detail before comparing the different ventilation concepts.

4.1. Detailed Discussion of one Concept

Before comparing the different ventilation concepts, we would like to discuss one ventilation concept in more detail: ceiling-based micro-jet ventilation with central and lateral exhaust at a volume flow rate of $\dot{V} = 13.3\,\mathrm{l/s/PAX}$ and a supply air temperature of $T_{supply} = 18.0\,°C$. For this selected ventilation concept, all investigated parameters are presented and discussed. These parameters are depicted in Fig. 6, which comprises two visualisations of the three-dimensional streamlines (a), temperature and velocity fields in a cross- and in a longitudinal section (b) and (c), the comfort-relevant quantities PMV (d), PPD (e), DR (f) and OT (g) for the central seat row as well as the age of air fields, again for a cross- and a longitudinal section (h). Due to the page limitation, not all corresponding figures for all ventilation concepts are going to be presented.

The three-dimensional streamline representations, see Fig. 6 (a), reveal that there is almost no longitudinal flow in the cabin leading to high homogeneity in longitudinal direction and high control efficiency. The latter offers the aircraft manufacturer and operator the opportunity to apply different temperature zones and to react on missing heat loads, that is, unoccupied seats. Further, the streamlines reveal that the supplied air flow constricts and follows the lateral overhead luggage compartments downwards where it splits up and a part of the air leaves the cabin through the lateral exhaust openings, while the other part follows the sidewall panels towards the floor. Here, the flow is redirected towards the centre of the cabin where it recirculates through the occupied zone. Partly, the flow leaves the cabin through the central exhaust and partly it mingles with the supplied air. This flow structure is also confirmed by the temperature (b) and velocity (c) cross-sections: cold air jets with high flow velocities are observed next to the lateral overhead compartments and the sidewall panels. The good homogeneity in longitudinal direction is also found, see right figures of (b) and (c), where the flow and temperature fields are almost independent on the considered seat row.

The comfort measures PMV and PPD (Fig. 6 (d) and (e)) reflect whether a passenger feels warm or cold and whether a passenger is dissatisfied with the thermal environment. For the considered ceiling-based ventilation with central and lateral exhausts, all passengers on the window seats and the legs of most of the other passengers are too cold. At the same time, some of the passengers sitting next to the aisle feel too warm in the head region. These too warm and too cold regions directly correlate with the regions where the passengers are more likely to be dissatisfied (e). Here local values of $PPD > 25\%$ are found.

The draught rate is depicted in Fig. 6 (f). High local values (>15%) are found in the leg room of the window benches and, particularly, on the window seats. The passengers on these window seats are directly influenced by the cold jets of fresh air,

which followed the lateral overhead compartments downwards. Here, the combination of cold air temperatures and high flow velocities induces very high, uncomfortable draught rates.
Fig. 6 (g) shows the operative temperature mapped on the enclosing surfaces of the thermal manikins. It can be interpreted as a "felt temperature" calculated based on the local heat flux and thus integrating the comfort-relevant quantities radiant temperature, ambient air temperature and air velocity. The operative temperature reflects warm head regions on the aisle seats and cold window seats for this ventilation concept. Since the PMV, see Fig. 6 (d), contains very similar information in a more intuitive representation:

- $-1.5 < PMV < -0.5$: cool
- $-0.5 < PMV < 0.5$: neutral
- $0.5 < PMV < 1.5$: warmish,

PMV will be used for further comparison of the different concepts in the next section.
Finally, we would like to discuss the local age of air displayed in Fig. 6 (h), which is an important quantity regarding the air quality. In the central cross-section (h), left, there are no age of air values above 90 s. Regarding the breathing zones of the seated passengers, the values are below 70 s expect for one aisle seat. These rather low values guarantee a sufficient supply of fresh air to all passengers. Looking at the longitudinal section (h), right, some increased values occur in the rear part of the cabin. These values are a result of the numerical boundary conditions in combination with the fact that the last seat row is very close to the non-permeable rear wall. However, these values also highlight that special attention has to be given to the last seat rows in front of non-permeable walls, such as galleys or toilet areas.

4.2. Comparison of all Ventilation Concepts

After this detailed discussion of all aspects of one selected velocity concept, we will now compare seven different ventilation concepts. Therefore, the ventilation concepts are divided into three groups: ceiling-based, floor-based and sidewall-based, see also Section 3. Within each group, the impact of different exhaust locations is analysed.
For the sake of brevity, we will show and discuss only the temperature (left) and velocity (right) fields obtained from the central cross-section for all of the different cases in Fig. 7 – Fig. 9. For the sake of comparability, we use the same legends for all cases.
Afterwards, the integral quantities, such as HRE, PMV and age of air, will be summarised and analysed in Tab. 2.
The first group of concepts consist of the ceiling-based ventilation systems, see Fig. 7. These are investigated at a volume flow rate of $10.0\ l/s/PAX$ and an inflow air temperature of 15.5 °C. Regarding the velocity fields, the first main finding is that the existence of a strong central exhaust, i.e. cases (c), reduces the maximal flow velocities next to the lateral overhead compartments significantly. Furthermore, the general flow fields for the two cases without central exhaust, (b) and (d), are very similar with only minor differences next to the lateral and dado exhausts. Here, the flow follows the lateral luggage compartments downwards towards the lateral or dado exhaust inducing two large circulations with upward flow in the central region of the cabin. In contrast to the cases without central exhaust where the maximal flow velocities occur next to the lateral overhead compartments, the concepts with an activated central exhaust, (a) and (c), reveal maximal velocities in the upper region of the aisle (c) and somewhat detached from the overhead compartments (a). As opposed to the concepts without central exhaust, (b) and (d), or weakly activated (a), we find reversed large-scale circulations with downward flow in the central region and with upward flow next to the side walls for case (c). As a consequence, we can conclude that the volume flow rate though the central exhaust determines the sense of rotation of the large-scale circulations in the cabin. Another fact to be noted is that the flow velocities within the seating zone are acceptably low for all cases except case (d), where the sole usage of the dado exhausts results in high flow velocities on and next to the window seats.

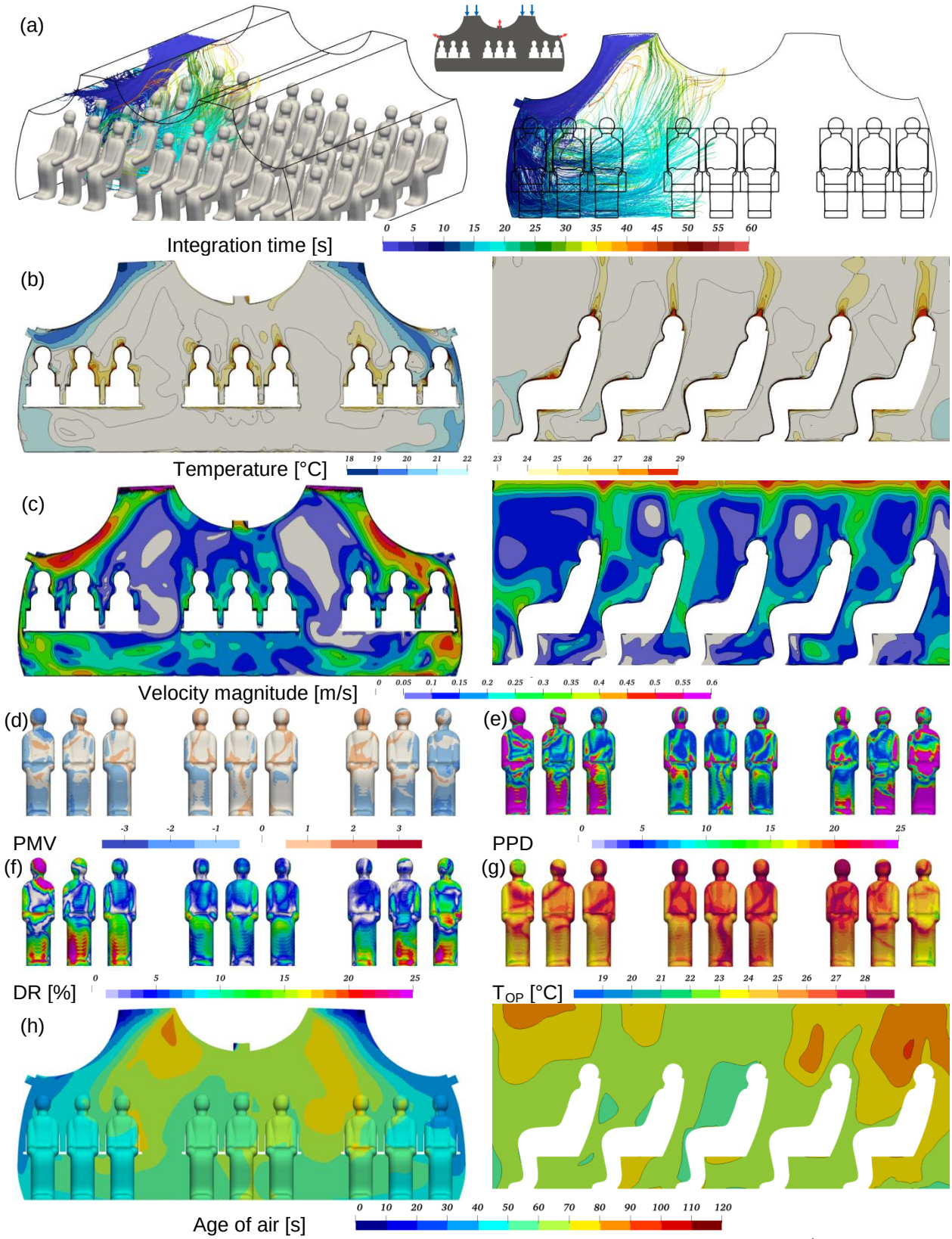

Figure 6. Detailed analysis of ceiling-based micro-jet ventilation with lateral and central exhaust @ $\dot{V} = 13.3\ l/s/PAX$ and $T_{supply} = 18.0\ °C$.

The temperature fields reflect the same main flow trends: The cases without central exhaust, (b) and (d), reveal very cold regions correlating with the high flow velocities. Especially for case (d), these will cause very uncomfortable draft. In contrast, the cases with active central exhaust, (a) and (b), reveal rather homogeneous, a little too cold, temperature distributions in the occupied area. Comparing these two cases with each other, further advantages are found for case (c) with central and dado exhausts activated.

The floor-based concept with fresh air supply from below is also known as cabin displacement ventilation. The drawbacks (higher required volume flow rate and high vertical temperature stratification) and advantages (very high heat removal efficiency, spatial homogeneity, low flow velocities and low risk of contaminant spreading) of this concept are already well known [2,13]. These are also confirmed by our numerical simulations: cabin displacement ventilation provides a temperature stratification with rather cold feet and a higher temperature on head level, see Fig. 8 left. Moreover, there is a high homogeneity, i.e. each the temperature and velocity distributions are independent on the choice of seat, and very low flow velocities can be observed, see Fig. 8 right. The latter is even more remarkable as a higher volume flow rate ($16.7\ l/s/PAX$), compared to all other investigated concepts, was applied. Due to the very high heat removal efficiency, see Tab. 2, higher inflow temperatures were used. Thus, the risk of cold draft is decreased and the energy demand of the environmental control system (ECS) is reduced further since the high-temperature bleed air must not be cooled down as much as for other concepts.

The last group of concepts to be discussed comprises the sidewall-based concepts. The fresh air is supplied through micro-jet elements integrated into the sidewall panels below the lateral luggage compartments. This concept, especially the case without central exhaust, see Fig. 9 (a), is comparable to classical mixing ventilation with lateral outlets only. As a consequence, we operated this ventilation concept with the standard $10\ l/s/PAX$ amount of fresh air and inflow temperatures of 16 °C. The first main finding for these concepts is that the activation of the central exhaust, case (b), has only a minor impact on the flow fields. This finding is a strong contradiction to the results obtained for the ceiling-based concepts, see Fig. 7, where the activation of the central exhaust strongly defines the main flow state. Further, the jet-like flow behaviour of the fresh air as a result of the constriction of the fresh air flow just after entering the cabin, induces flow velocities (much higher than 0.5 m/s). Maximal flow velocities below the lateral luggage compartments are as high as 1.1 m/s for the sidewall-based concepts (not resolved in the figures due to the choice of the legend for a higher comparability).

Regarding the temperature fields, the sidewall-based concepts reveal slightly cooler temperatures on the central seats, see Fig. 9, left. Surprisingly, the activation of the central exhaust leads to colder temperatures and higher flow velocities in the leg room of the passengers. Comparing the sidewall-based concepts with all other concepts, we identified that the cabin air flow is strongly determined by forced convection for this concept, while thermal convection – flow-induced by temperature gradients – plays an important role for all other concepts. Thereby, the floor-based concept is mainly driven by thermal convection. The ceiling-based concepts are a superposition of both driving mechanisms, forced and thermal convection.

Comparing all temperature and velocity fields of the different concepts, see Fig. 7 to Fig. 9, we identified the ceiling-based concept with central and dado exhaust as the most promising concept. It provides rather low flow velocities in the occupied zone, a rather homogeneous temperature distribution on almost all seats (only the windows seats are a little warmer) and a low risk of draft since no jets of cold air are found. However, the temperature level is in general a little too low for this case, which is also reflected in the integral PMV value given in Tab. 2.

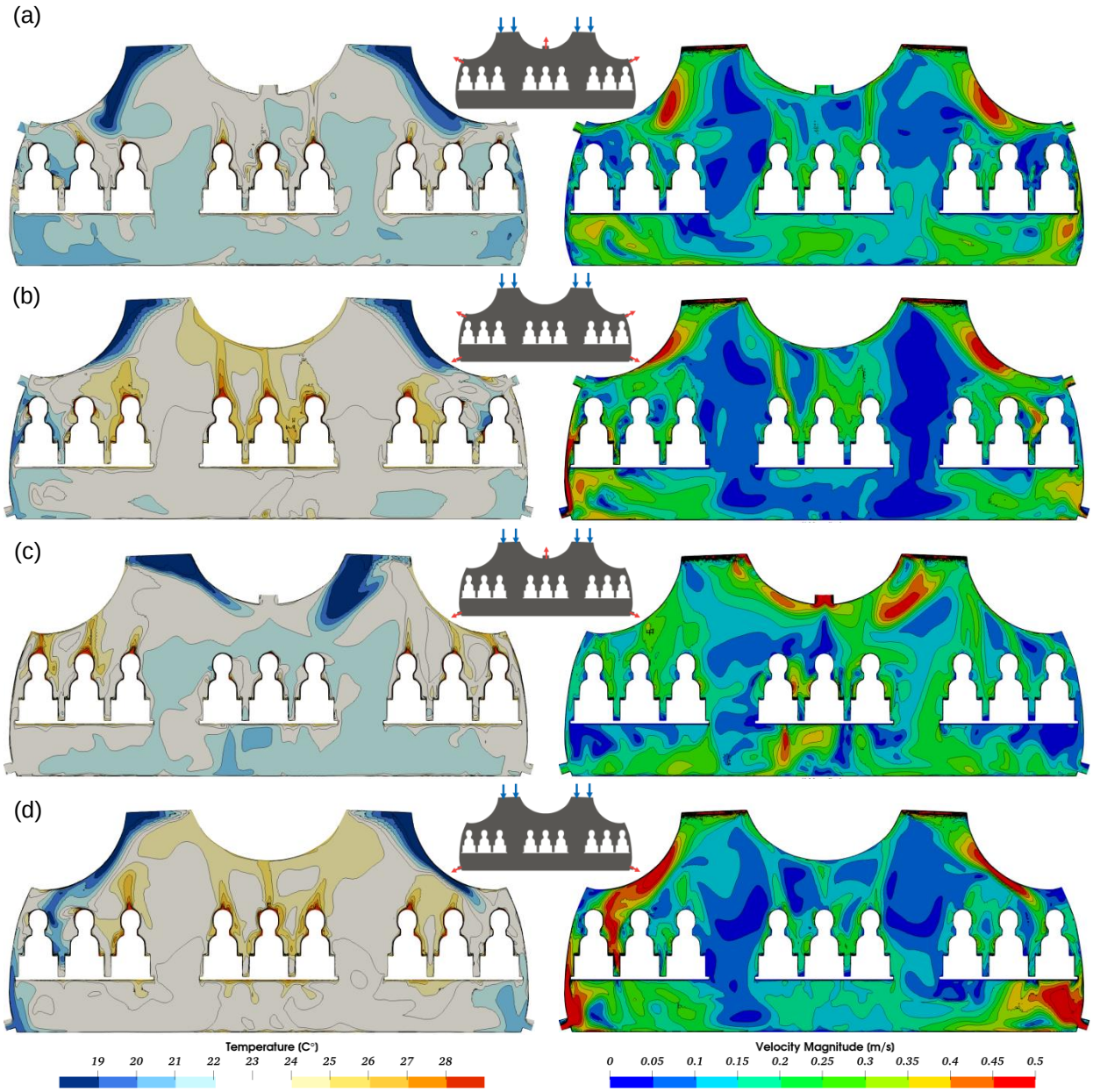

Figure 7. Temperature and velocity fields for ceiling-based concepts @ $\dot{V} = 10.0\ l/s/PAX$ and $T_{supply} = 15.5\ °C$. The legends at the bottom apply to all images.

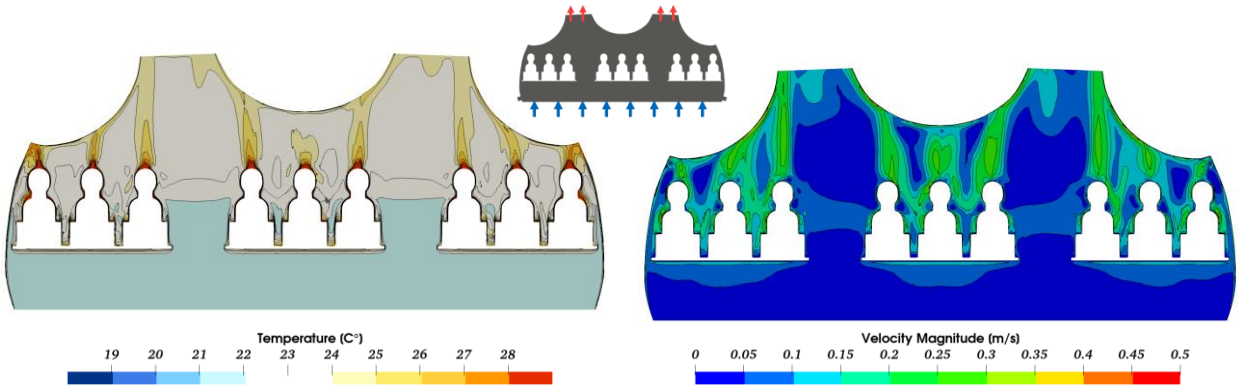

Figure 8. Temperature and velocity fields for floor-based concept @ $\dot{V} = 16.7\ l/s/PAX$ and $T_{supply} = 21.5\ °C$.

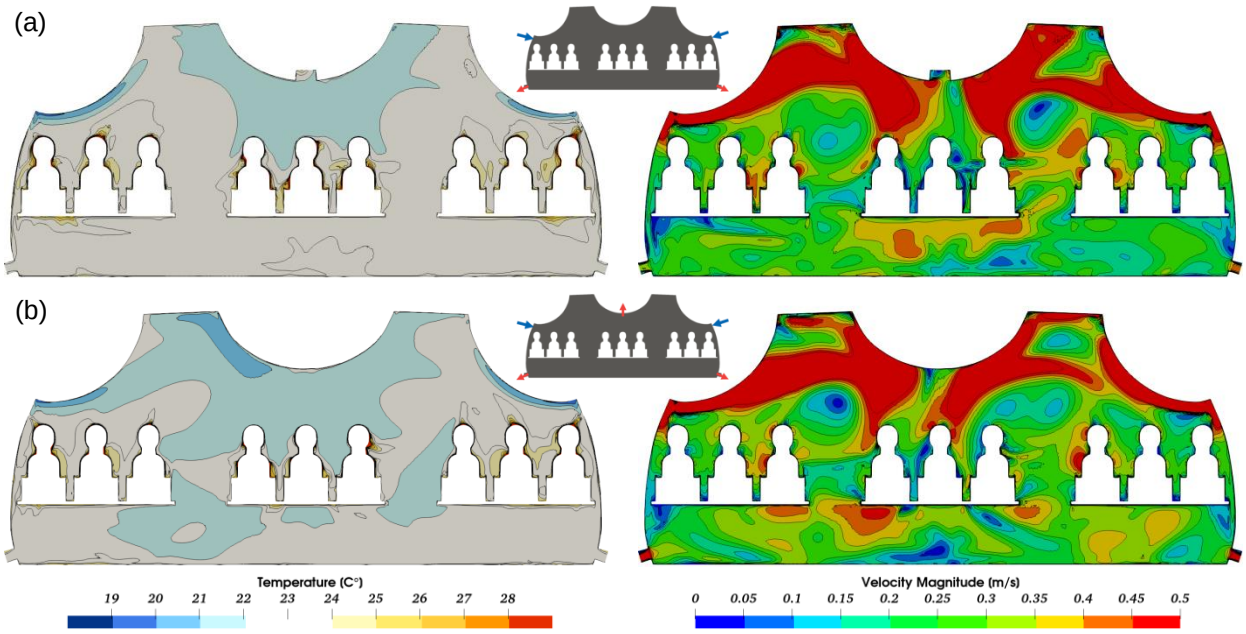

Figure 9. Temperature and velocity fields for sidewall-based concepts @ $\dot{V} = 10.0\ l/s/PAX$ and $T_{supply} = 16.0\ °C$. The legends at the bottom apply to all images.

Table 2. Integral / global quantities HRE, PMV and AoA for different ventilation concepts. *averaged over seating zone, **averaged over breathing zone.

Supply	Exhaust	HRE	$\langle PMV \rangle^*$	$\langle AoA \rangle^{**}$
Ceiling	Lat. + Centr.	0.55	- 0.24	74.1
Ceiling	Lat. + Dado	0.39	0.04	80.4
Ceiling	Centr. + Dado	0.49	- 0.11	75.3
Ceiling	Dado	0.37	0.05	87.0
Floor	Ceiling	1.05	0.21	49.8
Lateral	Centr. + Dado	0.52	- 0.22	40.7
Lateral	Dado	0.60	- 0.36	35.6

The global and integral quantities heat removal efficiency (HRE), predicted mean vote (PMV) and age of air (AoA) are summarised in Tab. 2. It must be noted, that the averaged PMV and age of air (AoA) values serve just as a guide. A detailed analysis of their maximal values and the number of seats above a certain threshold must be conducted in a second step.

Regarding the heat removal efficiency the floor-based concepts stands out. All other concepts are within a range of 0.60 to 0.37. Hereby, only the ceiling-based concepts with lateral and dado as well as with solely dado exhausts reveal HRE values below 0.4, which is the benchmark of classical state-of-the-art mixing ventilation [2]. As a consequence, we can summarise that most of the

novel ventilation concepts provide advantages over mixing ventilation regarding the heat removal efficiency.

Analysing the PMV values – averaged over the seating zone: $0.1\,m < z < 1.3\,m$ in the central cross section – we find very good values with $|PMV| < 0.4$ for all concepts. Here, the ceiling-based concepts with lateral and dado exhaust as well as with solely dado exhaust are almost perfectly neutral. Only the floor-based concept is a little too warm, while all other concepts are a little too cold. As stated above, a detailed analysis regarding the amount of seats or even amounts of body parts above a threshold must be conducted as next step.

The age of air values – averaged over the breathing zone: $0.9\,m < z < 1.3\,m$ in the central cross section – shows stronger variations. The lateral-based concepts reveal very good values around $40\,s$ being synonymous with very fresh air. However, these very low values are accompanied with high flow velocities, see Fig. 9. The age of air of the floor-based concept amounts to $50\,s$, which is also a very good value. All ceiling-based concepts reveal ages of air around $75 - 90\,s$ with the case with solely dado exhaust being the worst. Even though these values are the worst for all investigated novel ventilation concepts, they are still acceptable and will guarantee a sufficient supply of fresh air to the passengers.

5. EXPERIMENTAL VALIDATION IN NEW LONG-RANGE CABIN MOCK-UP

In addition to the numerical investigation of the ventilation concepts, a new test facility is constructed at DLR in Göttingen within the scope of the Clean Sky 2 financed ADVENT project. This new ground-based, full-scale test facility (mock-up) allows for experimental simulations and studies of future long-range cabin ventilation concepts with thermodynamically realistic boundary conditions and exceptionally homogeneous inflow conditions for unprecedented validation of CFD methods in subsequent projects. The mock-up has a length of 10 m and a width and height of up to 7 m and 3 m, respectively. In this mock-up, long-range cabin configurations can be realised. For the studies within the ADVENT project ten seat rows are installed. Special attention is given to the possibility to precisely define the thermal and fluid dynamical boundary conditions. This enables experimental simulations of different operational conditions (e.g. hot day on ground, climb and cruise) using temperature-controlled surfaces. While most of the existing studies of aircraft cabin ventilation just consider the performance under steady conditions, the dynamic performance is of high relevance under real conditions. Therefore, our investigations especially focus on the performance of the ventilation scenarios under dynamic conditions and non-ideal distributions of heat loads.

Further key features of the mock-up are its high modularity regarding the integration of different ventilation concepts and the preparation for the application of the latest measurement techniques, such as particle image velocimetry (PIV), thermal manikins, tracer gas analysis and others.

The new long-range cabin mock-up is presented and discussed in detail in the paper #022 entitled “New long-range cabin mock-up enabling the simulation of flight cases by means of tempered fuselage elements” [14] at this conference.

6. CONCLUSIONS and OUTLOOK

Numerical simulations were performed to analyze promising ventilation concepts in a simplified A350 geometry with nine-abreast seating. In a post-processing tool chain, thermal comfort quantities, such as predicted percentage of dissatisfied (PPD) and predicted mean vote (PMV) were calculated and the local mean age of air was determined. In total, seven different combinations of supply and exhaust locations were studied.

First main finding is that for the ceiling-based concepts the HRE decreases with the following order of exhausts: central + lateral, dado + central, dado + lateral to solely dado exhaust. Analysing this order reveals, that the HRE decreases with decreasing height of the exhaust for the ceiling based concepts. Regarding the HRE the floor-based concepts stands out with a value above 1, however, revealing strong, uncomfortable vertical temperature stratification.

Second main finding is that the flow rate through the central exhaust determines main flow characteristics for ceiling based concepts, whereas it has a negligible impact on the flow for lateral concepts. Regarding the physical driving mechanisms of the flow, we can conclude that the lateral concepts are dominated by forced convection while for all other concepts the thermal convection plays important role as well.

The age of air in the breathing zone reflects significant differences between the concepts: lowest values of around $40\,s$ are found for sidewall-based concepts. These are followed by the floor-based concept and finally the ceiling-based concepts reveal with around $75 - 90\,s$ the

worst, but still acceptable age of air values. The analysed PMV values are all within the very good range of $|PMV| < 0.4$. However, detailed analysis for single seats or even single body parts should be conducted in the future.
Within the framework of the ADVENT project, we will install different novel ventilation concepts in the new cabin mock-up starting with ceiling-based concepts. Experimentally and numerically, these concepts will be analysed and detailed solutions regarding orientation and technical realisation will be developed. Subsequently, further novel concepts will be analysed solely and in combination with other comfort-enhancing techniques.

7. CLOSING REMARK

This project has received funding from the Clean Sky 2 Joint Undertaking under the European Union's Horizon 2020 research and innovation programme under grant agreement No 755596.

Further, the authors would like to thank Annika Köhne for proof-reading the manuscript.

8. REFERENCES

1. Kühn, M., Bosbach, J. & Wagner, C. (2009). Experimental parametric study of forced and mixed convection in a passenger aircraft cabin mock-up. *Build. Environ.* **44**, 961-970.

2. Bosbach, J., Lange, S., Dehne, T., Lauenroth, G., Hesselbach, F. & Allzeit, M. (2013). Alternative ventilation concepts for aircraft cabins. *CEAS Aeronaut J.* **4**(3), 301-313.

3. Modest M. F., (2013). Radiative Heat Transfer, 3rd ed., *Academic*, New York.

4. Patankar, S. & Spalding, D. (1972). A Calculation Procedure for Heat, Mass and Momentum Transfer in Three-dimensional Parabolic Flows. *Int. J. Heat and Mass Transfer* **15**, p. 1787.

5. ISO 7730:2005 (2005). Ergonomics of the thermal environment - Analytical determination and interpretation of thermal comfort using calculation of the PMV and PPD indices and local comfort criteria. International Standard Organization.

6. Fanger, P. (1970). Thermal Comfort, *Danish Technical Press*, Copenhagen, Denmark.

7. Fanger, P., Melikov, A. & Ring, J., (1988). Air turbulence and sensation of draught. *Energy and Buildings* **12**, pp. 21-39.

8. ENGYS, (2018). HELYX®3.1.0 | HELYX-Core User's Guide.

9. Bartak, M., Cermak, M., Clarke, J. A.,Denev, J., Drkal, F., Lain, M., Macdonald, I. A., Majer, M., Stankov, P., (2001). Experimental and numerical study of local mean age of air. *Seventh international IBPSA Conference 2001*.

10. Wick, A. (2011). Ventilation Efficiency and Thermal Comfort, Airbus: Internal Report Ref: N21D10027368.

11. DB Systemtechnik (2018). [Online] Available at: https://www.db-systemtechnik.de/resource/blob/1665152/b1e975afc4621103696b63e8247d37ce /Aktuell_D_Schulbrosch%C3%BCre-Regensburg_Das-System-Bahn---der-ICE-data.pdf (accessed June, 13th 2018).

12. Schmeling, D., (2019). Neue Belüftungs-konzepte und individuelle Komfortzonen im Schienenverkehr (in German). *In BAHN-TECHNIK AKTUELL* (Band 72 / 2019) Proceedings of the ECO-RAIL-HVAC 2019, IFV Bahntechnik e.V., Berlin, Germany.

13. Bosbach, J., Heider, A., Dehne, T., Markwart, M., Gores, I. & Bendfeldt, P. (2012). Evaluation of cabin displacement ventilation under flight conditions. *In Proceedings of the ICAS 20212*, Brisbane, Australia.

14. Schmeling, D., Lange, P., Dehne, T., Dannhauer, A., Werner, F. & Gores, I., (2020). New long-range cabin mock-up enabling the simulation of flight cases by means of tempered fuselage elements. *In Proceeding of the Aerospace Europe Conference 2020*, Paper #022, Bordeaux, France.